

CuO/TiO₂/γ-Al₂O₃ 催化剂表征及对 NO+CO 反应性能研究

李惠娟 蒋晓原* 张 旭 郑小明

(浙江大学理学院化学系催化研究所, 杭州 310028)

摘要: 采用色谱-微反流法反应装置考察了 $w\%$ CuO/15% TiO₂/γ-Al₂O₃ 催化剂对 NO+CO 的反应活性; 催化剂经空气氛或氢气氛预处理后, NO 转化率达 100% 的反应温度分别是 325 和 275 °C; XRD 仅能检测到 γ-Al₂O₃ 晶相, 负载 15% CuO 后可以检测到微弱的 CuO 晶相; H₂-TPR 能检测到 2 个 CuO 的还原峰(α 和 β 峰), 将其归属于高度分散的 CuO 分别在裸露的 γ-Al₂O₃ 和 TiO₂/γ-Al₂O₃ 载体上的还原; 原位红外分析结果表明催化剂经空气氛或氢气氛预处理后, 吸附 NO+CO 反应气后, 反应的中间产物 N₂O 出现的温度分别为 200 和 150 °C。

关键词: CuO-TiO₂/γ-Al₂O₃; NO+CO 反应; NO+CO 吸附; 原位红外表征

中图分类号: O614.41; O614.121; O611.62

文献标识码: A

文章编号: 1001-4861(2008)06-0848-08

Characterization and Catalytic Properties of CuO/TiO₂/γ-Al₂O₃ for NO+CO Reaction

LI Hui-Juan JIANG Xiao-Yuan* ZHANG Xu ZHENG Xiao-Ming

(Institute of Catalysis, Department of Chemistry, Faculty of Science, Zhejiang University, Hangzhou 310028)

Abstract: The catalytic activity and properties of $w\%$ CuO/15% TiO₂/γ-Al₂O₃ in NO+CO reaction were examined using a micro-reactor gas chromatography reaction system. When pretreated by air and H₂, the catalysts had 100% NO conversion at 325 and 275 °C, respectively. The XRD analysis could only detect γ-Al₂O₃ crystal diffraction and weak CuO crystal diffraction peaks after 15% CuO loading. There were two H₂-TPR reduction peaks in CuO-TiO₂/γ-Al₂O₃, the α peak due to the highly dispersed CuO which spread on γ-Al₂O₃ surface and the other peak due to the highly dispersed CuO which dispersed on 15% TiO₂/γ-Al₂O₃ surface. The DRIFTS analysis showed that catalysts with pretreatment in air or H₂ atmosphere adsorbed NO+CO gases, and the N₂O adsorption peaks appeared at 200 and 150 °C, respectively.

Key words: CuO-TiO₂/γ-Al₂O₃; NO+CO reaction; NO+CO adsorption; DRIFTS characterization

The emission of NO_x from both mobile and fixed stationary sources is a serious environmental problem because it causes the formation of smog, acid rain, global warming and depletion of the stratospheric ozone layer^[1-3]. It is urgent to eliminate NO_x pollution and improve environmental quality^[4-12]. A lot of studies suggest that TiO₂ catalysts have more unique intrinsic activities than γ-Al₂O₃ catalysts^[13-15]. However, low spe-

cific surface area and poor thermal stability restrict the widespread use of titania as a catalyst support. To overcome these shortcomings, many mixed oxides containing TiO₂ (e.g. TiO₂-SiO₂, TiO₂-ZrO₂ and TiO₂-γ-Al₂O₃) were synthesized^[16-19].

CuO is a good catalytic component for eliminating NO_x. When CuO is loaded on the TiO₂-mixed oxides, it has excellent catalytic activity for the

收稿日期: 2007-09-23。收修改稿日期: 2008-03-04。

浙江省自然科学基金(No.Y504131)资助项目。

*通讯联系人。E-mail: xyjiang@mail.hz.zj.cn; Tel: 0571-88273283

第一作者: 李惠娟, 女, 30 岁, 博士研究生; 研究方向: 多相催化与环境催化。

removal of NO_x^[20,21]. Amano et al^[22] investigated the activity of CuO/γ-Al₂O₃ in NO+CO reaction and found that the catalyst had high one-electron reducibility (Cu²⁺→Cu⁺), suggesting the redox enhanced NO+CO reaction. Luo Mengfei et al^[23] prepared CuO/γ-Al₂O₃ catalysts at different CuO loadings by impregnation method, and found that the activity of CuO/γ-Al₂O₃ in CO oxidation increased with CuO loading. Jiang et al^[24] examined the activities of CuO/TiO₂ using a fixed-bed continuous flow reactor and reported 99% NO conversion at 325 °C after pretreatment with H₂ at 500 °C for 2 h.

In this study, high specific surface area TiO₂/γ-Al₂O₃ was synthesized by co-precipitation method. The catalytic properties and activity of CuO/TiO₂/γ-Al₂O₃ in NO+CO reaction were examined using the XRD, TPR and FTIR techniques.

1 Experimental

1.1 TiO₂/γ-Al₂O₃ preparation

TiO₂/γ-Al₂O₃ was synthesized by co-precipitation method. First Al(NO₃)₃·9H₂O crystallite was dissolved in double distilled water to prepare 3.0 mol·L⁻¹ Al(NO₃)₃ aqueous solution and then slowly added to 0.1 mol·L⁻¹ TiCl₄ solution. With vigorous stirring, the dilute NH₃·H₂O(1:1, v/v) was dropped into the mixed solution until pH=10.5. The precipitation was laid in the solution for 24 h, then washed with distilled water until free from Cl⁻ ions. The solid materials were dried at 110 °C overnight and calcined at 500 °C for 2 h, after that, cooled to room temperature in air to obtain the TiO₂/γ-Al₂O₃ mixed oxide.

1.2 Catalyst preparation

CuO/TiO₂/γ-Al₂O₃ catalysts were prepared by wetness impregnation method. An amount of Cu(NO₃)₂ aqueous solution was added to TiO₂/γ-Al₂O₃ to yield certain metal loading. All the catalysts were dried at 110 °C in oven overnight and calcined at 500 °C for 2 h, denoted as w% CuO/15% TiO₂/γ-Al₂O₃, where w% and 15% represent the weight percentage of CuO and TiO₂, respectively.

1.3 Catalytic activity in NO+CO reaction

Catalytic activity was determined under the steady

state in a fixed-bed quartz reactor (Φ=5 mm). The reaction gas consisted of 6.0%NO, 6.0%CO and 88%He (V/V). 60 mg of catalyst with particle size of 40~60 mesh (420~250 μm) was used. The reactions occurred at different temperatures with a space velocity of 1 000 0 h⁻¹. The analysis of the gases concentration in the reactor effluent was performed using a gas chromatography (GC) equipped with a TCD detector (the detector temperature was 200 °C). A molecular sieve 13X column (2 m×4 mm×0.30 μm, stainless steel, controlled at 40 °C) was used to separate N₂, NO and CO, and a Paropak Q column(2 m×4 mm×0.33 μm, stainless steel, controlled at 40 °C) to analyze N₂O and CO₂. the GC carrier gas was H₂ and its flow rate was 25 mL·min⁻¹.

1.4 Catalytic characterization

X-ray diffraction (XRD) data were obtained using a horizontal Rigaku B/Max III B powder diffractometer with Cu Kα radiation(λ=0.154 18 nm) obtained by using Ni filter and a power of 40 kV×30 mA. The diffraction angles were 2θ(20°~70°).

H₂-temperature programmed reduction (TPR) was done by the GC method using a thermal conductivity detector. Sample was put into a quartz tube, with 95% N₂ and 5%H₂ mixtures(V/V) at flow rate of 15 mL·min⁻¹. After the base line was stabilized, temperature increased at a rate of 10 °C·min⁻¹.

Specific surface area was determined by the BET method with N₂ adsorption at the liquid-nitrogen temperature using Coulter OMNISORP-100CX instrument. The samples were degassed in vacuum(10⁻⁵ Pa) for 2 h at 200 °C.

Transmission electron microscopy(TEM) was done on a JEOL JEM-2010 (HR) microscope at 200 kV, The powder was ultrasonically suspended in alcohol for 5 min, and the suspension was deposited on a copper grid previously covered with a thin layer of carbon, and the TEM observations were carried out after drying the mesh.

FTIR experiments were performed using Nicolet 560 spectrometer with a MCT detector and a high-pressure, high temperature DRIFTS cell (Thermo Spectra-Tech) fitted with ZnSe windows. Spectra were acquired at a resolution of 4 cm⁻¹ typically averaging

100 scans. The sample was pretreated in oxygen or hydrogen at 400 °C for 1 h, then cooled down to room temperature in the same gas to obtain the background. The oxygen or hydrogen was pumped off, and the absorbed gas was led to the IR cell. All spectra were taken at different temperatures. The flow rate through the IR cell was 15 mL·min⁻¹. The absorbed gas contained 10%NO+90%He, 10%CO+90%He or 6%NO+6%CO+88%He(V/V).

2 Results and discussion

2.1 Specific surface areas of TiO₂/γ-Al₂O₃ and w% CuO/15% TiO₂/γ-Al₂O₃

Specific surface areas of w% CuO/15% TiO₂/γ-Al₂O₃ decrease with CuO loading (Table 1). The pore structure data and 15% TiO₂/γ-Al₂O₃ catalysts calcined at different temperatures are shown in Table 2. Specific surface area is the largest after TiO₂/γ-Al₂O₃ is calcined at 500 °C and changes little from 600 to 700 °C, but decreases with further increase in calcination temperature, which is consistent with previous studies^[25]. After TiO₂/γ-Al₂O₃ is calcined at high temperature, from the TEM micrograph, we can see that the particles of TiO₂ and Al₂O₃ are enlarged and aggregated with increasing in calcination temperature, many pores are disappeared and the spacing of particles grows larger, this may result in the great specific surface area decreasing. The

Table 1 Specific surface areas at different loadings of w% CuO/15% TiO₂/γ-Al₂O₃ (500 °C, 2 h)

| CuO / % | 0 | 3 | 6 | 9 | 12 | 15 |
|--|-----|-----|-----|-----|-----|-----|
| Specific surface area / (m ² ·g ⁻¹) | 266 | 246 | 206 | 192 | 179 | 165 |

Table 2 Specific surface areas of TiO₂/γ-Al₂O₃ calcined at different temperatures

| Temperature / °C | 500 | 600 | 700 | 800 | 900 | 1 000 |
|---|-------|-------|-------|-------|-------|-------|
| Specific surface areas/(m ² ·g ⁻¹) | 266 | 196 | 199 | 142 | 100 | 45 |
| Pore volume / (mL·g ⁻¹) | 0.352 | 0.349 | 0.413 | 0.396 | 0.390 | 0.138 |
| Average pore size / nm | 9.42 | 9.75 | 10.48 | 12.53 | 16.76 | 23.74 |
| Volume adsorbed / (mL·g ⁻¹) (STP) | 61.09 | 43.26 | 45.65 | 32.73 | 23.06 | 9.36 |

evolution of pore structure is strongly affected by calcination temperature. In all cases, the average pore size increases with increasing calcination temperature. For the most of materials, surface area reduction accompanies the pore size increase due to the removal of materials from the convex grain to the more concave necks. After calcinations at 500 to 900 °C, the average pore sizes are 9.42 nm, 9.75 nm, 10.48 nm, 12.53 nm, 16.76 nm, respectively. This results are in the same trend as the study of Choi et al^[26].

2.2 TEM results

TEM is also employed to observe the shape and the size of the 15% TiO₂/γ-Al₂O₃ mixed oxides calcined at 500 and 1 000 °C for 2 h(Fig.1). From the two micrograph, we can see that there are many pores dispersed on the 15% TiO₂/γ-Al₂O₃ mixed oxides calcined at 500 °C. But for the 15% TiO₂/γ-Al₂O₃ calcined at 1 000 °C, the sintering of TiO₂ and Al₂O₃ particles are detected, a lot of pores of the mixed oxide are disappeared. We think that the structure of the TiO₂/γ-Al₂O₃ mixed oxide aggregates and collapses with increasing calcined temperature, and then produces large space among the primary particles. The TEM results agree well with our BET results.

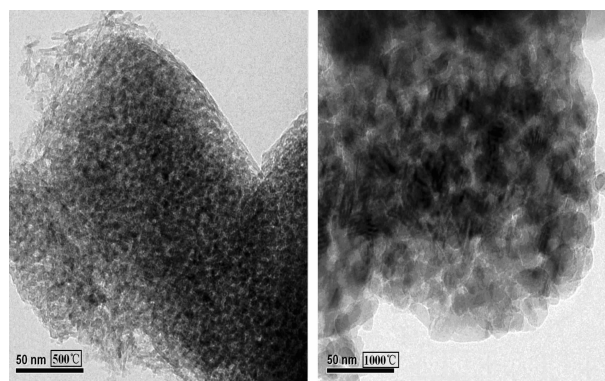
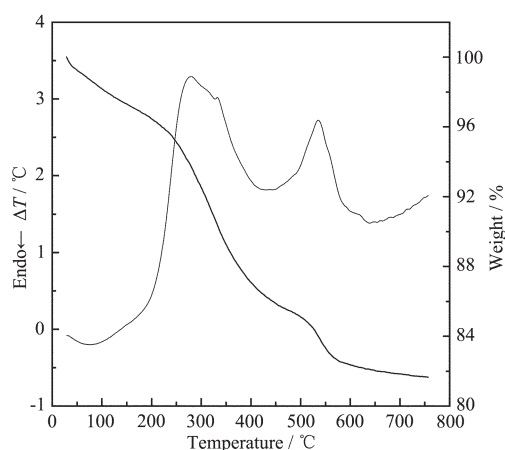


Fig.1 TEM micrograph of the 15%TiO₂/γ-Al₂O₃ calcined at 500 °C and 1 000 °C for 2 h

2.3 TG-DTA results

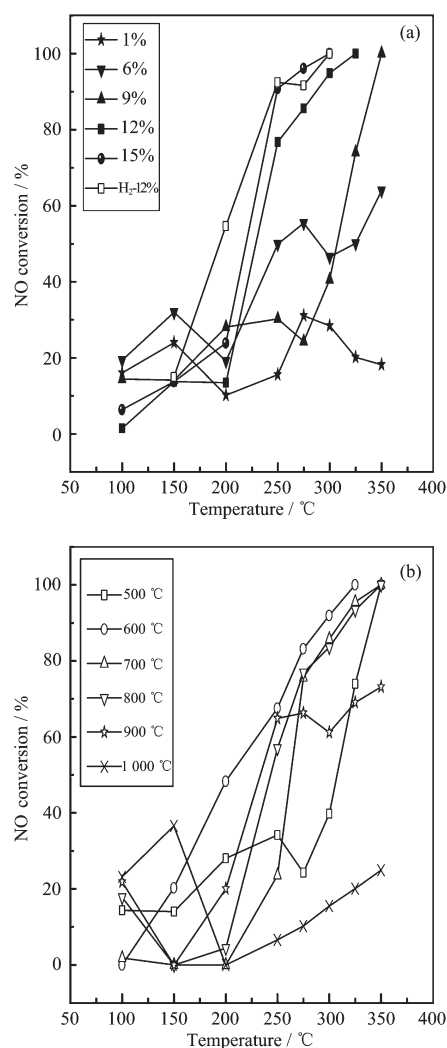
The DTA profile show three endothermic peaks at around 90, 440 and 600 °C (Fig.2), corresponding to three weight losses in the TG curve. According to the literature^[27], it is presumed that the 90 °C peak is due to the removal of physically absorbed water molecules. The 440 °C peak is the result of phase transformation of boehmite to γ-Al₂O₃, and the peak at 600 °C is deemed

Fig.2 TG-DTA curves of TiO₂/γ-Al₂O₃

to the γ-Al₂O₃ phase formed completely^[28].

2.4 Catalytic activity of NO

The activity of *w*% CuO/15% TiO₂/γ-Al₂O₃ with different CuO loadings calcined at 500 °C for 2 h are shown in Fig.3a. From the curve, it can be observed that there is a twist for every catalysts appeared at 150 ~ 200 °C except for the catalyst pretreated by H₂. We speculate that this phenomena is caused by NO adsorption and desorption on the catalysts. Compared with FTIR spectra in section 2.7, a lot of NO molecules could adsorbed on the catalysts at low temperatures, which results in very quick increase in NO conversion from 100 to 150 °C. However, with increasing the temperature, the NO molecules desorbe from the catalyst, and the detected NO conversion decreases, thus bringing about a twist. But when the reaction temperature continues to increase, the NO+CO reaction initializes, this can also be seen from FTIR spectra in section 2.7, the intermediate products N₂O become larger at 200 °C. Then the NO conversion goes up rapidly from 200 °C on. Because there may be some difference in the NO adsorption and desorption on different catalysts, the temperature range for twists to appear might not be the same. When talking about the reaction temperature from 200 to 400 °C, it could be seen that the NO conversion increases rapidly with temperature. And the more CuO loading, the lower temperature for the total NO conversion. According to our XRD results, there is no CuO phase detected from *w*% CuO/15% TiO₂/γ-Al₂O₃ (500 °C, 2 h) catalysts. And our TPR has merely one peak



(a) *w*%CuO/15%TiO₂/γ-Al₂O₃ catalysts with different CuO loadings;
(b) 12%CuO/15%TiO₂/γ-Al₂O₃ calcined at different temperatures

Fig.3 Activity of catalysts in NO+CO reaction

for all catalysts, we suggest that the highly dispersed CuO might be the NO+CO reaction active component. When the catalysts has higher CuO loading, there are more highly dispersed CuO, so they have better catalytic activity. As for the catalyst pretreated by H₂ at 400 °C for 1 h, the catalytic activity increases and its 100% NO conversion temperature is 300 °C, and at the same time the twist at 200 °C is also disappeared. There might be two reasons responsible for the above observations. The catalysts have adsorbed H₂ during pretreatment with H₂ at 400 °C for 1 h. According to Lietti et al^[29], H₂ could evolve in the NO+CO reaction, the NO elimination is a reduction reaction, and the desorption of H₂ favors for the reductions, thus decreasing the temperature for 100%

NO conversion. Similar results were also reported by Wu et al^[30].

For the catalysts calcined at different temperatures, 12%CuO/15%TiO₂/γ-Al₂O₃ (600 °C, 2 h) has the highest activity in NO+CO reaction, with 100% NO conversion at 325 °C (Fig.3b). Although catalysts calcined at 500, 700 and 800 °C have some differences in catalytic activity at low temperature, they all reach 100% NO conversion at 350 °C. However, when the catalyst is calcined at 900 °C for 2 h, 100% NO conversion occurs at 450 °C, and for the catalyst calcined at 1 000 °C only has lower than 20% NO conversion at 450 °C. In general, w%CuO/15%TiO₂/γ-Al₂O₃ catalysts have better thermal stability, despite a limitation of calcination temperature. The best calcination temperature is 600 °C.

2.5 H₂-TPR results

Our previous work showed a strong reduction peak at 356 °C for CuO, two reduction peaks at 240 and 289 °C for 12%CuO/γ-Al₂O₃, and two reduction peaks at 318.9 and 387.5 °C for 12% CuO/TiO₂^[31]. In this study, there is no reduction peak for 15%TiO₂/γ-Al₂O₃, but a broad reduction peak (α=250 °C) appears when 3%CuO is loaded (Fig.4). As CuO loading increases, the α peak becomes larger, especially for the 12% and 15% CuO loading catalysts. As for 6%, 9%CuO loading, the

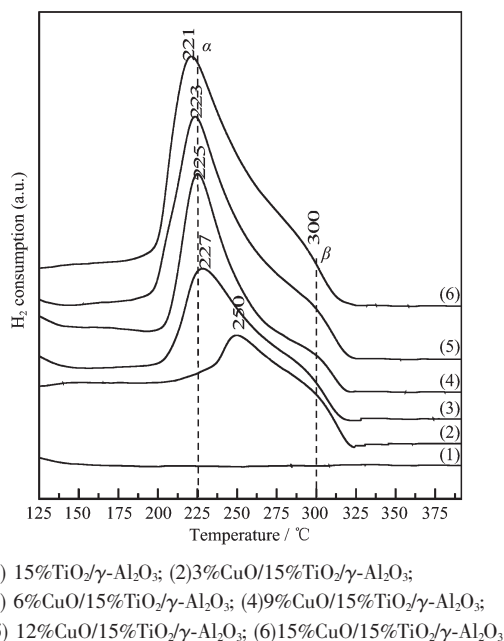
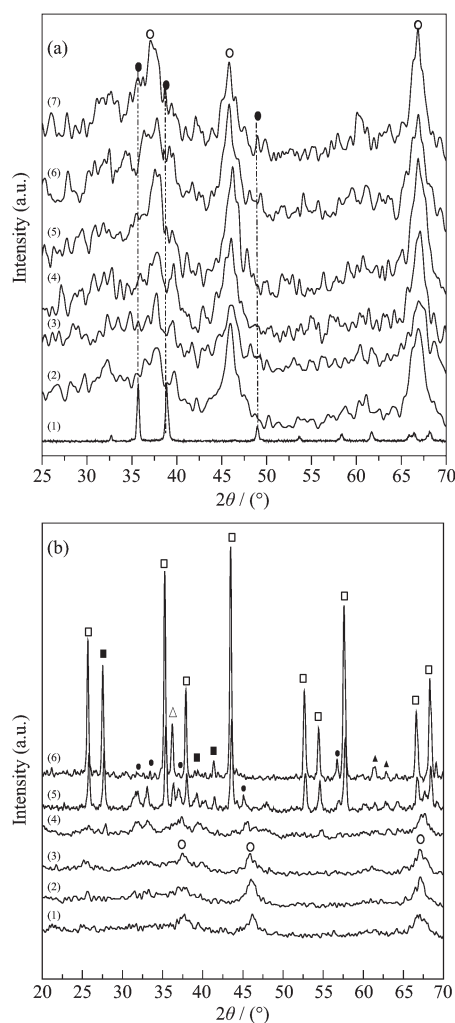


Fig.4 H₂-TPR profiles of catalysts calcined at 500 °C for 2 h

other reduction peak (β=300 °C) appears. From XRD results, there is no CuO phase for the most of catalysts, so these two peaks might be due to the reduction of highly dispersed CuO catalysts. According to Xu et al^[32] and our previous result, we assign this α peak to the highly dispersed CuO on γ-Al₂O₃ surface, the other β peak due to the highly dispersed CuO on 15%TiO₂/γ-Al₂O₃ surface.

2.6 XRD results

With increasing CuO loading, the XRD patterns of w% CuO/15% TiO₂/γ-Al₂O₃ change little and TiO₂ crystallite diffraction peaks are not detected, but γ-Al₂O₃ diffraction peaks are observed (Fig.5a). Weak CuO



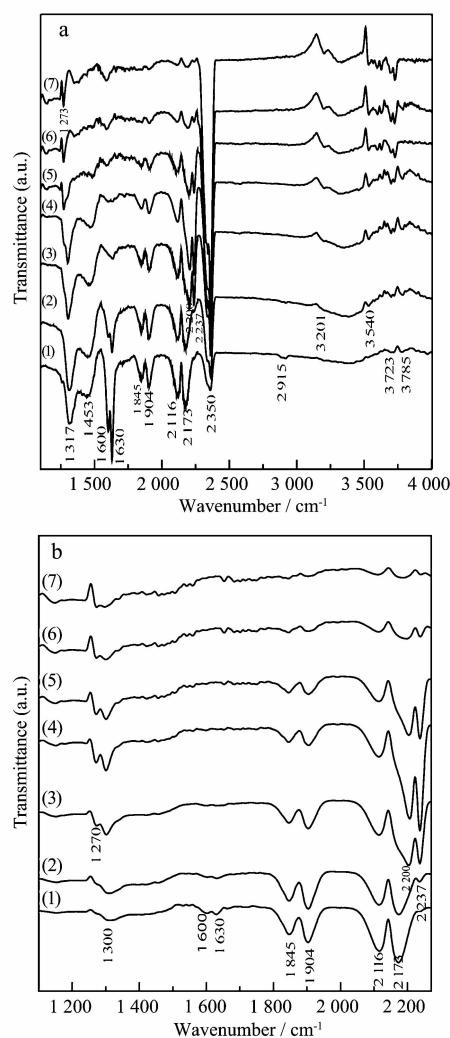
w%CuO/TiO₂/γ-Al₂O₃ with different CuO loadings (a): (1) CuO; (2) 0%; (3) 3%; (4) 6%; (5) 9%; (6) 12%; (7) 15% (● CuO ○ γ-Al₂O₃) and TiO₂/γ-Al₂O₃ calcined at different temperatures (b): 100 °C; (2) 600 °C; (3) 700 °C; (4) 800 °C; (5) 900 °C; (6) 1 000 °C (■ rutile TiO₂, ▲ TiAl₂O₃, ○ γ-Al₂O₃, □ α-Al₂O₃, △ δ-Al₂O₃, ● θ-Al₂O₃)

Fig.5 XRD patterns of catalysts

diffraction peaks are detected only for 15% CuO/15% TiO₂/γ-Al₂O₃. When TiO₂/γ-Al₂O₃ is calcined at low temperature, γ-Al₂O₃ diffraction peaks are detected without a trace of TiO₂ diffraction peaks (Fig. 5b). Calcined at 900 °C, many diffraction peaks of TiO₂ rutile phase are observed. It is known that titania mainly exists in two forms, anatase and rutile, with transformation temperatures at the range of 600~800 °C^[34]. For 15%TiO₂/γ-Al₂O₃, the transformation temperature increases to 900 °C, indicating that the addition of TiO₂ to γ-Al₂O₃ increases TiO₂ transformation temperature. It is common that TiO₂ anatase phase helps catalyze the NO+CO reaction. The preparation of 15%TiO₂/γ-Al₂O₃ by co-precipitation might have improved thermal stability. When 15%TiO₂/γ-Al₂O₃ is calcined at 900 °C, δ-Al₂O₃ and θ-Al₂O₃ phases appear and γ-Al₂O₃ phase weakens. Calcined at 1 000 °C, the α-Al₂O₃ phase is observed.

2.7 DRIFT analysis

Under flow of reaction mixture NO (6%) and CO (6%) in balance with He, DRIFT spectra taken over 12%CuO/15%TiO₂/γ-Al₂O₃ catalysts at different temperatures are shown in Fig. 6a. The catalyst was first oxidized in O₂ at 400 °C for 1 h and then cooled to 25 °C before exposing to the reaction mixture. The bands at 1 845 cm⁻¹ is attributed to Cu(I)-NO species and 1 904 cm⁻¹ due to Cu(II)-NO. As the surface temperature increases, the peak intensities of NO adsorption bands decrease gradually. After the sample contacts with NO+CO at 100 and 200 °C, the Cu²⁺ sites are reduced and, as a result, no Cu²⁺-CO(2 192 cm⁻¹^[35]) species are detected. Scarano et al^[36] suggested that Cu⁺(CO)₂ species were produced during low-temperature CO adsorption on Cu/SiO₂, and they proposed a band at ca. 2 115 cm⁻¹ to correspond to ν_{as} and ν_s, a band at ca. 2 160 cm⁻¹ to the modes of the Cu⁺(CO)₂ species. According to these literatures, we propose that the bands at 2 116 and 2 173 cm⁻¹ are assigned to the ν_{as} and ν_s of Cu⁺(CO)₂ species. The different results given here could be due to the lower interaction temperature and/or the different support and sample preparation technique. The 2 116 cm⁻¹ peak intensity decreases with temperature but the 2 173 cm⁻¹ peak becomes smaller at 150 °C



(1) 100 °C; (2) 150 °C; (3) 200 °C; (4) 250 °C;
(5) 300 °C; (6) 350 °C; (7) 400 °C
(a) pretreated by air for 1 h at 400 °C;
(b) pretreated by H₂ for 1 h at 400 °C

Fig.6 DRIFTS spectra of 12%CuO/15%TiO₂/γ-Al₂O₃ absorbing NO+CO

and disappears at 200 °C. At the same time a new peak at 2 200 cm⁻¹ appears. 2 352 cm⁻¹ band belongs to the CO₂ adsorption and its intensity becomes larger with temperature. 1 630, 2 915 and 3 540 cm⁻¹ are due to stretching vibrations of O-C-O, C-H and O-H, respectively. These three bands might be caused by the HCOOH(CO+H₂O→HCOOH) existed on the surface of catalysts^[37]. The bands at 1 600 cm⁻¹ are NO₂ adsorption peaks. And the bands at 1 270, 1 300 cm⁻¹ are assigned to monodentrate and bidentrate symmetric stretching vibrations of the NO_x (x=2~3)^[38]. These three peaks (1 600, 1 270 and 1 300 cm⁻¹) weaken rapidly with

temperature. The N_2O adsorption peak ($2\,237\text{ cm}^{-1}$) appears at $200\text{ }^\circ\text{C}$, it goes bigger at $250\text{ }^\circ\text{C}$ and becomes smaller and smaller when the surface temperature of catalysts is higher than $300\text{ }^\circ\text{C}$.

At low temperatures, $12\%\text{ CuO}/15\%\text{ TiO}_2/\gamma\text{-Al}_2\text{O}_3$ had NO and CO adsorption peaks are at the same location regardless of pretreatments by air or H_2 (Fig. 5b) at $400\text{ }^\circ\text{C}$ for 1 h. The peak at $1\,600\text{ cm}^{-1}$ is weak, indicating only a few NO_2 species. The peaks at $1\,270$, $1\,300\text{ cm}^{-1}$ are also small, and NO_3^- peak at $1\,430\text{ cm}^{-1}$ is not detected. When $12\%\text{ CuO}/15\%\text{ TiO}_2/\gamma\text{-Al}_2\text{O}_3$ is pretreated by air at $400\text{ }^\circ\text{C}$ for 1 h, there are more oxygen species on the catalyst surface. The oxygen species react with NO+CO gases at low temperature to produce NO_2 , NO_x and nitrate species. However, pretreatment by H_2 at $400\text{ }^\circ\text{C}$ for 1 h offers fewer oxygen species on the catalyst and therefore produces fewer NO_x species. At $200\text{ }^\circ\text{C}$ the bands at $2\,173\text{ cm}^{-1}$ disappear but $2\,210\text{ cm}^{-1}$ adsorption peak appears. The N_2O band at $2\,237\text{ cm}^{-1}$ appears at $150\text{ }^\circ\text{C}$, becomes the strongest at $250\text{ }^\circ\text{C}$, weakens at $350\text{ }^\circ\text{C}$, then disappears at $400\text{ }^\circ\text{C}$. It is suggested that the N_2O intermediates are produced at low temperature, then turned into N_2 at higher temperature.

There have been many studies on the band peak at $2\,210\text{ cm}^{-1}$. Tamás Bánsági et al.^[39] investigated the adsorption of NO+CO gases by Rh/CeO₂ using FTIR techniques and assigned the band peak $2\,210\text{ cm}^{-1}$ to Rh-NCO⁻ species adsorption. Venezia et al.^[40] studied the coadsorption of NO+CO on Pd/SiO₂ catalysts, and assigned $2\,190\text{ cm}^{-1}$ band to Pd(-NCO). According to other authors^[41,42], the $2\,150\sim 2\,200\text{ cm}^{-1}$ adsorption bands belong to M-NCO species (M denotes metal or metal ions). Therefore when CO and NO are co-absorbed by the transition metal or the transition metal oxides at higher temperatures, NCO⁻ usually is produced. By analogy with the results of Beloshapkin et al.^[43], they assigned the bands at $2\,205\text{ cm}^{-1}$ to the asymmetric stretching of $\text{Cu}^+\text{-NCO}$ species. In this study, the $2\,210\text{ cm}^{-1}$ adsorption peak appears at $200\text{ }^\circ\text{C}$ or higher temperatures, where CO reduces CuO into Cu^0 and Cu^+ , and we only test the $\text{Cu}^+(\text{CO})_2$ species. Above all, we attribute the band at $2\,210\text{ cm}^{-1}$ to the $\text{Cu}^+\text{-NCO}^-$ spec-

ies adsorption.

After $12\%\text{ CuO}/15\%\text{ TiO}_2/\gamma\text{-Al}_2\text{O}_3$ is pretreated by H_2 atmosphere, few oxygen species exist on the surface of catalyst and thus less NO_x and nitrate are produced in NO+CO reaction. Because N_2O is a very important intermediate in the NO+CO reaction, its appearing and disappearing temperatures could directly influence the rate of NO+CO reaction and NO conversion. This study has explained why catalysts pretreated by H_2 have higher activity than those pretreated by air atmosphere.

3 Conclusions

(1) $w\%\text{ CuO}/15\%\text{ TiO}_2/\gamma\text{-Al}_2\text{O}_3$ catalysts have high catalytic activity and thermal-stability for NO+CO reaction, the reaction temperature is $325\text{ }^\circ\text{C}$ in air and $275\text{ }^\circ\text{C}$ in H_2 for 100% NO conversion over $12\%\text{ CuO}/15\%\text{ TiO}_2/\gamma\text{-Al}_2\text{O}_3$ ($500\text{ }^\circ\text{C}$, 2 h).

(2) $15\%\text{ TiO}_2/\gamma\text{-Al}_2\text{O}_3$ catalysts prepared by coprecipitation method have high BET surface area, its pore size increases with temperature. Only $\gamma\text{-Al}_2\text{O}_3$ crystallite diffraction peaks are detected and weak CuO crystal diffraction peaks could be detected for $15\%\text{ CuO}$ loading for $w\%\text{ CuO}/15\%\text{ TiO}_2/\gamma\text{-Al}_2\text{O}_3$ ($500\text{ }^\circ\text{C}$, 2 h). Two TPR peaks (α , β) are detected when CuO is loaded on $\text{TiO}_2/\gamma\text{-Al}_2\text{O}_3$. The α and β peak are assigned to the highly dispersed CuO reduction on $\gamma\text{-Al}_2\text{O}_3$ and $15\%\text{ TiO}_2/\gamma\text{-Al}_2\text{O}_3$, respectively.

(3) After catalysts are pretreated in air and H_2 atmosphere, DRIFT analysis detects the N_2O adsorption peaks in NO+CO reaction at $200\text{ }^\circ\text{C}$ and $150\text{ }^\circ\text{C}$, respectively.

References:

- [1] Pasel J, Speer V, Albrecht C, et al. *Appl. Catal. B: Environ.*, **2000**, **25**:105~133
- [2] Dandclear A, Vannice M A. *Appl. Catal. B: Environ.*, **1999**, **22**:179~200
- [3] Fino D, Russo N, Saracco G. *J. Catal.*, **2006**, **242**:38~47
- [4] Chupin C, Veen A C V, Konduru M. et al. *J. Catal.*, **2006**, **241**:103~114
- [5] Shelef M. *Chem. Rev.*, **1995**, **95**:209~225
- [6] Ramis G, Busca G, Bregani F, et al. *Appl. Catal.*, **1990**, **64**:259~278

- [7] Koebel M, Elsener M, Kleemann M. *Catal. Today*, **2000**,**59**: 335~345
- [8] Wang J A, Cuan A, Salmones J, et al. *Appl. Surf. Sci.*, **2004**, **230**:94~105
- [9] Crucq A. (Ed.), *Catalysis and Automotive Pollution Control II, Study of Surface Science and Catalysis*, Vol.71. Amsterdam: Elseiver, **1991**.
- [10] Ciuparu D, Bensalem A, Pfefferle L. *Appl. Catal. B: Environ.*, **2000**,**26**:241~245
- [11] Ozkan U S, Kumthekar M W, Karakas G. *Catal. Today*, **1998**, **40**:3~14
- [12] Ali A, Alvarez W, Loughran C. *J. Appl. Catal. B: Environ.*, **1997**,**14**:13~22
- [13] Li W, Li S X, Zhang M H, et al. *Colloids and Surfaces A: Physicochem. Eng. Aspects*, **2006**,**272**:189~193
- [14] Ramírez J, Macías G, Cedeño L, et al. *Catal. Today*, **2004**,**98**: 19~25
- [15] Maity S K, Ancheyta J, Soberanis L, et al. *Appl. Catal. A*, **2003**,**244**:141~153
- [16] Santes V, Herbert J, Cortez M T, et al. *Appl. Catal. A*, **2005**, **281**:121~128
- [17] Dhar G M, Srinivas B N, Rana M S, et al. *Catal. Today*, **2003**, **29**: 4~45
- [18] Masakazu A, Takafumi K, Sukeya K. *J. Phys. Chem.*, **1988**, **92**:438~440
- [19] Wei Z B, Xin Q, Guo X X, et al. *Appl. Catal.*, **1991**,**75**:179~191
- [20] Yahiro H, Iwamoto M. *Appl. Catal. A*, **2001**,**222**:163~181
- [21] Parvulescu V I, Grange P, Delmon B. *Catal. Today*, **1998**,**46**: 233~316
- [22] Amano F, Suzuki S, Yamamoto T, et al. *Appl. Catal. B: Environ.*, **2006**,**64**:282~289
- [23] Luo M F, Fang P, He M, et al. *J. Mol. Catal. A: Chem.*, **2005**, **239**:243~248
- [24] Jiang X Y, Ding G H, Lou L P, et al. *J. Mol. Catal. A: Chem.*, **2004**,**218**:187~195
- [25] Hordern B K. *Adv. Colloid Interface Sci.*, **2004**,**110**:19~27
- [26] Junseo C, Jinsoo K, Kye S Y, et al. *Powder Technology*, **2007**,**180**:83~88
- [27] Iwamoto M, Yahiro H, Torikai Y. *Chem. Lett.*, **1990**:1967~1970
- [28] LIU Hua(刘 华), SHI Zhong-Hua(史忠华), CHEN Yao-Qiang(陈耀强), et al. *Chinese. J. Inorg. Chem. (Wuji Huxue Xuebao)*, **2004**,**20**:688~692
- [29] Lietti I N L, Tronconi L C E, Forzatti P. *J. Catal.*, **2006**,**239**: 244~254
- [30] Wu Y, Zhao Z, Liu Y, et al. *J. Mol. Catal. A: Chemical*, **2000**, **155**:89~100
- [31] LI Hui-Juan(李惠娟), JIANG Xiao-Yuan(蒋晓原), ZHENG Xiao-Ming(郑小明). *Acta Phys.-Chim. Sin. (Wuli Huaxue Xuebao)*, **2006**,**22**:584~589
- [32] Xu B, Lin D, Chen Y. *J. Chem. Soc., Faraday Tran.*, **1998**,**94**: 1907~1918
- [33] Vargas A, Montoya A, Maldonado C, et al. *Micropor. Mater.*, **2004**,**74**:9~17
- [34] Giakoumelou I, Fountzoula C, Kordulis C. et al. *J. Catal.*, **2006**,**236**:1~12
- [35] Venkov T, Hadjiivanov K. *Catal. Commun.*, **2003**,**4**:209~213
- [36] Scarano D, Bordign S, Lamberti C, et al. *Surf. Sci.*, **1998**,**411**: 27~34
- [37] Li J H, Ke R, Li W, et al. *Catal. Today*, **2007**,**126**:272~278
- [38] Cordoba G, Viniegra M, Fierro J L G, et al. *Solid State Chem.*, **1998**,**138**:1~6
- [39] Tamás B, Tímea S Z, Frigyes S. *Appl. Catal. B: Environ.*, **2006**,**66**:147~150
- [40] Venezia A M, Liotta L F, Deganello G. *Langmuir*, **1999**,**15**: 1176~1181
- [41] Sica A M, Gigola C E. *Appl. Catal. A: Gen.*, **2003**,**239**:121~139
- [42] Larsson P, Andersson A, Wallenberg L R, et al. *J. Catal.*, **1996**,**163**:279~293
- [43] Beloshapkin S A, Paukshtis E A, Sadykov V A. *J. Mol. Catal. A: Chem.*, **2000**,**158**:355~359